The Role of Attractive Dispersion Interaction in Promoting The Catalytic Activity of Asymmetric Hydrogenation

Journal:	*Organic Chemistry Frontiers*
Manuscript ID	QO-HIG-03-2023-000332.R5
Article Type:	Research Article
Date Submitted by the Author:	08-Jun-2023
Complete List of Authors:	Yang, Limin; Hangzhou Normal University, College of Materials, Chemistry & Chemical Engineering Li, Bo; California Institute of Technology, Division of Chemistry and Chemical Engineering Houk, K.; University of California Los Angeles, Department of Chemistry

ARTICLE

The Role of Attractive Dispersion Interaction in Promoting The Catalytic Activity of Asymmetric Hydrogenation

Received 00th January 20xx,
Accepted 00th January 20xx

DOI: 10.1039/x0xx00000x

Limin Yang,*[ab] Bo Li,[c] and K. N. Houk*[b]

As an essential van der Waals interaction, the dispersion interaction is an important weak attractive interaction. However, the influence of the weak attractive intereactions has only recently been elucidated in transition metal catalyzed asymmetric hydrogenations by the Wanbin Zhang group. Our IGM/EDA analysis proves Zhang's finding that attractive interactions play an important role in asymmetric hydrogenation, which provides new strategies for the sophisticated design of chiral transition metal catalysts. The dispersion interaction is the major weak attractive interaction that activates the asymmetric hydrogenations by favorable interactions of substrate and metal catalyst.

Introduction

Attractive dispersion interactions, a van der Waals interaction also called London dispersion interactions, have only recently been studied in organic reactions because of the development of practical computational methods to compute such interactions.[1] Recently, dispersion interactions have been recognized to play an important role in influencing reactivity and stereoselectivity in enzyme- and organo-catalyzed asymmetric reactions.[1-4] However, the significant effects of attractive dispersion interactions between substrate and ligand have been described only in a few homogeneous transition-metal catalyzed asymmetric transformations.[5-6]

Transition-metal catalyzed asymmetric hydrogenation of unsaturated substrates is one of the most important transformations for preparing chiral products. Over the past half century, numerous catalysts based on chiral ligands coordinated with noble-metals have been designed, synthesized, and evaluated for catalytic selectivity and efficiency, and a series of highly efficient asymmetric hydrogenation reactions have been developed.[7] Although some noble-metals, such as Rh, Ru, and Ir, catalyzed asymmetric hydrogenations have been applied in industry, their high cost and toxicity have prevented them from broad application.[8]

In order to control the cost and reduce the toxicity of chiral catalysts in asymmetric hydrogenations, earth-abundant transition metal catalysts have been considered as alternatives due to their abundance, low cost, and environmental friendliness. However, compared with asymmetric hydrogenation catalyzed by noble-metals, their catalytic efficiency is generally very low, and they have not been used in industry.[9]

To tackle the challenges mentioned above, Wanbin Zhang group at Shanghai Jiao Tong University has improved significantly the catalytic efficiency of the earth-abundant transition metal nickel catalyzed asymmetric hydrogenations by exploiting attractive weak interactions between the ligand and substrate existing in the key transition state structure. This group published a series of papers in *Angew. Chem.*, *Nat. Commun.* and *Nat. Chem.*, describing their discoveries.[10-16] In these studies, weak attractive interactions have been found to play an important role by stabilizing the favorable key transition state structure formed by chiral catalysts and substrates and promoting the hydrogenation reaction. These weak attractive interactions could be found as CH···HC, CH···π, CH···O, and other interactions in Zhang and his coworkers' work. However, after summarizing these works, we believe there is a key interaction dominating the weak interaction, therefore, a series of analysis has been proceeded and proved the dispersion interaction as the major weak interaction.

Results and discussion

At first, IGM[17,18] (Independent Gradient Model) analysis has been carried out to identify the location of the interactions based on the Wanbin Zhang group's original DFT computational structures. It should be noted that IGM methods are inspired by the RDG approach (also known as NCI analysis),[19] and intermolecular interactions do not interfere with intramolecular interactions in IGM unlike RDG analyses.[17] The figure notes and graphic symbols of IGM analysis are listed in Figure 1.

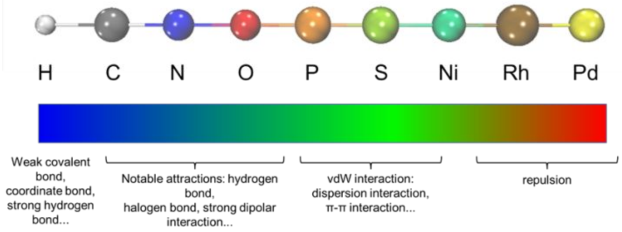

Figure 1. Figure notes and graphic symbols of IGM analysis.

---

[a] College of Material, Chemistry and Chemical Engineering, Hangzhou Normal University, Hangzhou, Zhejiang 311121, China. E-mail: myang@hznu.edu.cn

[b] Department of Chemistry and Biochemistry, University of California, Los Angeles, CA 90095-1569, USA. E-mail: houk@chem.ucla.edu

[c] Division of Chemistry and Chemical Engineering, California Institute of Technology, Pasadena, CA 91125, USA.

Second, we performed EDA (Energy Decomposition Analysis) to identify the specific weak interaction quantitatively.[20] This EDA is aimed at the interaction between substrate and metal complex. The total interaction energy, marked as E_{total}, has been divided into six parts: the electrostatic interaction (E_{ele}), the exchange repulsion interaction (E_{ex}), the induction interaction (E_{ind}), the dispersion interaction (E_{disp}), the distortion of substrate ($E_{dist(sub)}$), and the distortion of metal complex ($E_{dist(cat)}$). In general, the total interaction energies E_{total} are always negative and the relative level of energies are corresponded to the free energies in the manuscript. E_{ele} (always positive) represents the coordination interaction in these computations, E_{ind} (always negative) represents interaction between dipole and induced dipole like C-H...O or C-H...π, and E_{disp} (always negative) represents interaction between instantaneous dipoles like C-H...H-C. $E_{dist(sub)}$ and $E_{dist(cat)}$ represent distortion of substrate and the distortion of metal complex respectively, which are always positive. According to these studies, dispersion interactions (CH...HC interactions) have the potential to enhance the reactivity of hydrogenations, resulting in a high S/C (Substrate/Catalyst, mole ratio) value and in some cases the stereoselectivity.

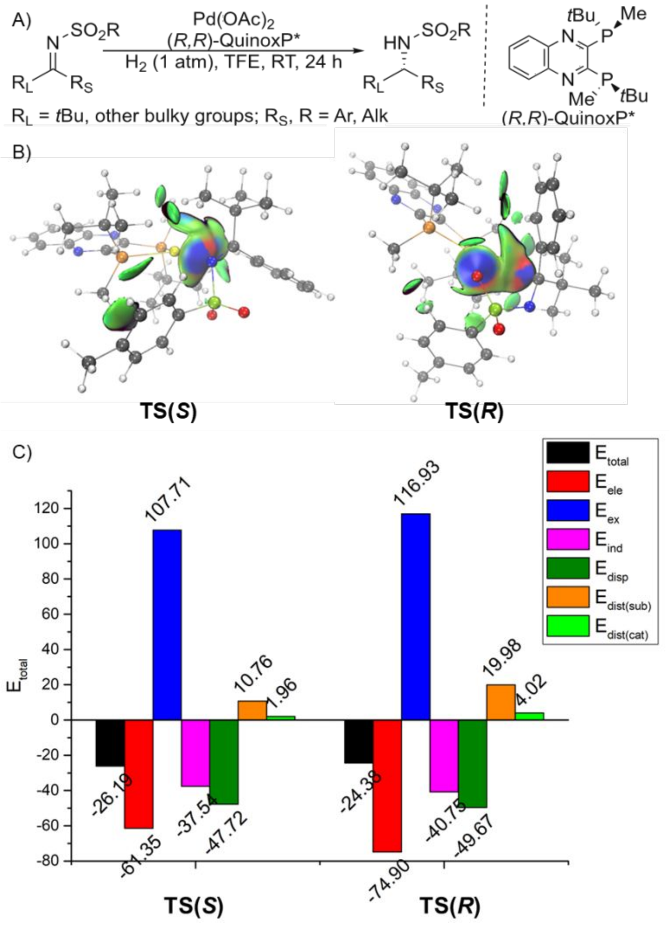

Figure 2. A) Hydrogenation of *N*-sulfonyl imines; B) IGM analysis of **TS(*S*)** and **TS(*R*)**; C) EDA analysis of **TS(*S*)** and **TS(*R*)**.

Compared with the noble-metal Rh, Ru, and Ir catalysts, only a few efficient Pd-catalyzed asymmetric hydrogenations have been reported. In 2018, W. Zhang and coworkers initially reported a highly efficient $Pd(OAc)_2$-catalyzed asymmetric hydrogenation of sterically hindered *N*-sulfonyl imines (Figure 2A).[10] By employing a cheap palladium salt $Pd(OAc)_2$ with low toxicity and (*R*,*R*)-QuinoxP* as ligand, highly catalytic activity and enantioselectivity were observed (up to 99% yield, 99% ee, and 5000 S/C) in the reaction. In the ligand screening of the reaction, normal aryl-substituted diphosphine ligand with axial chirality like (*R*)-BINAP gave no desired product. Only by using alkyl-substituted phosphine ligands, the reaction would occur. And the yield increased as the increase of the substituents of the alkyl groups.

In Zhang's report, computational investigation and control experiments revealed that the high catalytic efficiency originates from the significant structural differences caused by weak attractive interactions between the catalyst and substrate. Our IGM and EDA analysis further shows the existing of strong and significant attractive dispersion interactions (Figure 2B), with the large E_{disp} (compared with E_{ind}) in the EDA (Figure 2C). The dispersion interactions could be found both in **TS(*R*)** and in **TS(*S*)**, thus increase the reactivity efficiently. Even though **TS(*S*)** with the lower activation energy in Figure 2 has a relatively weaker attractive dispersion interaction (E_{disp} = -47.72 kcal/mol) than that of **TS(*R*)** (E_{disp} = -49.67 kcal/mol), without these dispersion interactions, the reaction does not occur smoothly. These IGM/EDA analyses indicated the dominance of dispersion interactions, and was consistent with the experimental data mentioned above.

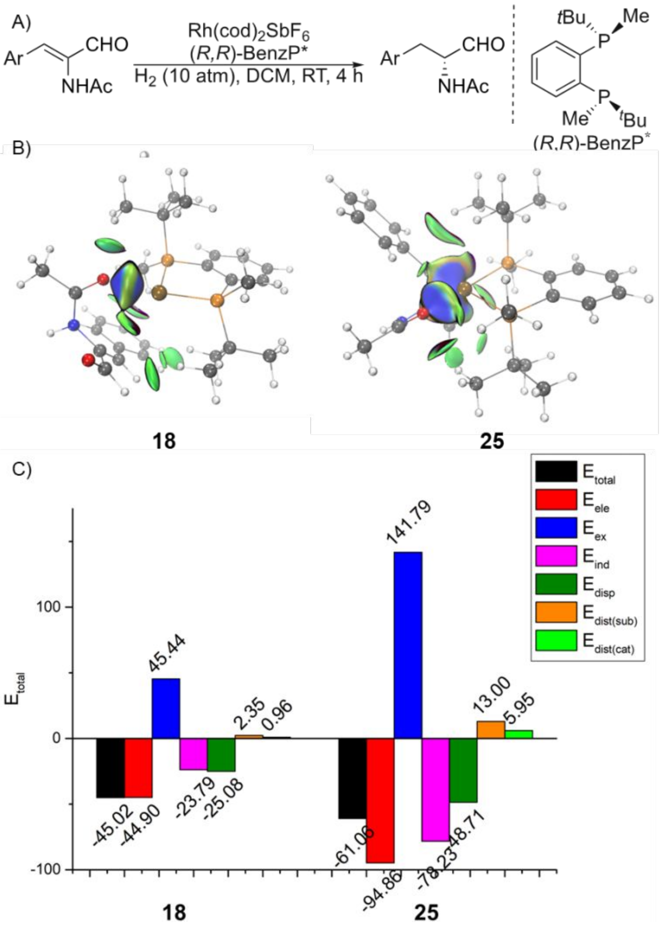

Figure 3. A) Hydrogenation in α-formyl enamides; B) IGM analysis of **18** and **25**; C) EDA analysis of **18** and **25**.

Chiral α-amino aldehydes have a wide range of potential applications in organic synthesis and medicinal chemistry. To synthesize chiral α-amino aldehydes with high efficiency, W. Zhang and coworkers reported a highly efficient Rh-catalyzed asymmetric hydrogenation of *α*-formyl enamides using BenzP* as ligand, affording chiral *α*-amino aldehydes with up to 20000 S/C.[11] Again, normal aryl-substituted diphosphine ligand with axial chirality like (*R*)-BINAP gave no desired product. Yet the reaction occurs with alkyl-substituted phosphine ligands. Zhang's DFT computational investigation revealed that the weak interactions between the ligand and substrate are the crucial features in the formation of key intermediates (Figure 3A). The IGM shows the interactions between substrates and metal catalyst (Figure 3B). However, our further EDA analysis shows a different view of weak interactions (Figure 3C). In intermediate **25**, the E_{ind} dominates the weak interactions. However, this intermediate is too stable and hardly reacts, only leading to unfavored product. For the actual reacted intermediate **18**, dispersion interactions promote the hydrogenation. These analyses indicated the dominance of dispersion interactions, and are consistent with the experimental data mentioned above.

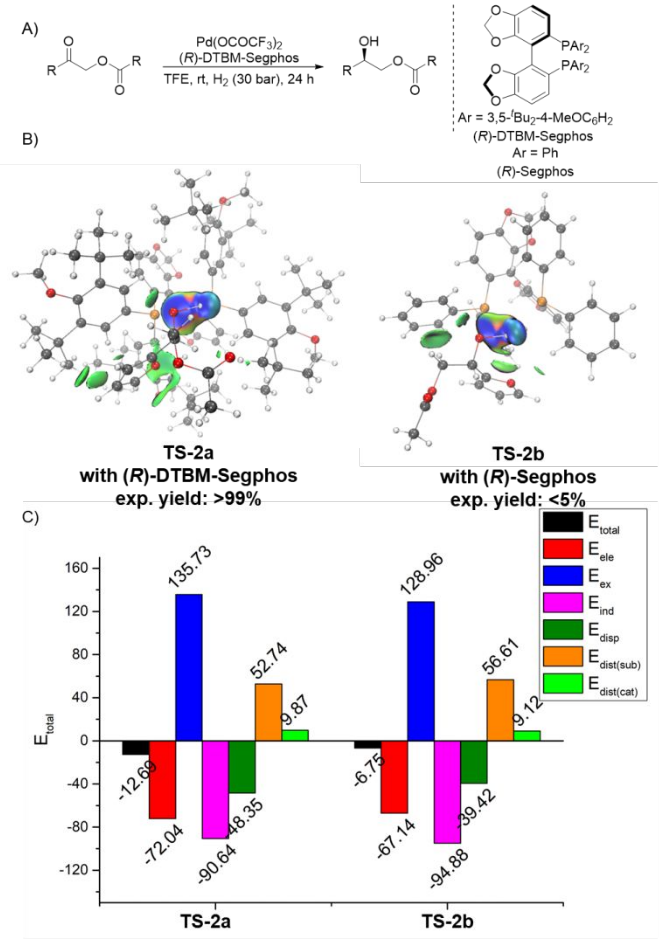

Figure 4. A) Hydrogenation in α-acyloxy-1-arylethanones; B) IGM analysis of **TS-2a** and **TS-2b**; C) EDA analysis of **TS-2a** and **TS-2b**.

Zhang's coworkers, Chen and D. Gridnev studied the weak interactions in catalytic hydrogenation with DFT in 2020.[21] They studied the asymmetric hydrogenation of α-acyloxy-1-arylethanones via Pd and (*R*)-DTBM-Segphos, studied by Zhang and coworkers in 2013 (Figure 4A).[22] This example compared the energy barrier of hydrogenation with (*R*)-DTBM-Segphos and (*R*)-Segphos. With (*R*)-DTBM-Segphos which is considered to have large steric hindrance, the energy barrier was about 7.6 kcal/mol lower than with (*R*)- Segphos, that does not have the two bulky tert-butyl groups. The result matched the experimental yield of standard substrate >99% (with (*R*)-DTBM-Segphos) and <5% (with (*R*)-Segphos) respectively.

According to the IGM analysis, there are more attractive dispersion interactions in **TS-2a**, especially near the *tert*-butyl groups of (*R*)-DTBM-Segphos. In **TS-2b**, fewer attractive dispersion interactions are found (Figure 4B). The enantioselective step is the heterolysis of H_2, and the EDA shows large induction interaction energies and high distortion energies of substrate. However, these do not affect the analysis of attractive dispersion interactions. With *tert*-butyl groups the E_{disp} of **TS-2a** is -48.4 kcal/mol, much larger than the E_{disp} of **TS-2b** -39.5 kcal/mol (Figure 4C). Dispersion also contributes most to the decrease of the activation energy (See SI, Table S3).

Based on the above mentioned Pd- and Rh-catalyzed asymmetric hydrogenations utilizing weak attractive interactions, Zhang's group turned to the first-row earth-abundant transition metal nickel catalyzed asymmetric hydrogenations. They reported an efficient earth-abundant metal nickel catalyzed asymmetric hydrogenation of *N*-sulfonyl imines almost at the same time as the previous investigations (Figure 5A). The active (*R*,*R*)-QuinoxP*-Ni complex existing in the equilibrium to excess $Ni(OAc)_2$ improved the hydrogenation efficiency and provided chiral *t*-Bu-sulfonyl amines with high yields and excellent enantioselectivities (up to 99% yield and 99% ee).[12] A dramatically decreased catalyst loading (10500 S/C) represents the best catalytic behavior for the reported nickel-catalyzed asymmetric hydrogenations. Similarly, normal aryl-substituted diphosphine ligand with axial chirality like (*S*)-BINAP or (*S*)-Segphos gave desired product with low yield (51% and 38%, respectively). By introducing *tert*-butyl group in the P atom of the phosphine ligand, the reaction proceeded smoothly. Larger version of (*S*)-Segphos, (*S*)-DTBM-Segphos can also promote the reaction, though the selectivity was not satisfactory (58%). Nevertheless, these results indicate the importance of dispersion interactions. According to Zhang's DFT computational investigation, dispersion interactions play an essential role in the high catalytic efficiency and excellent enantioselectivity origination. The quantitative difference of CH···HC interactions was found between the *R*- and *S*-transition state structures, partly accounting for the results, and revealing the effect of the *tert*-butyl group. The IGM analysis shows multiple dispersion interactions around the *tert*-butyl group, revealing its importance in the combination of the catalyst with substrates (Figure 5B).

Also, our further EDA shows that the dispersion interaction is the major weak interaction in **TS(*R*)**, significantly stronger than that in **TS(*S*)** (-47.74 kcal/mol vs -25.89 kcal/mol, Figure 5C). According to the IGM analysis of **TS(*R*)**, the *tert*-butyl of substrate shows obvious interaction with the *tert*-butyl in the ligand, while lesser interactions are found in **TS(*S*)** (Figure 5B), consistent with Zhang's results as well. In this example, dispersion interaction not only improved the reactivity but also the enantioselectivity of the asymmetric hydrogenation reaction. On this basis, W. Zhang also developed the efficient Ni-catalyzed asymmetric hydrogenations for the synthesis of α-phenylalanines and α-phenylglycines.[13,14] In these cases, only when using alkyl-substituted phosphine, especially *tert*-butyl substituted ligands, the reaction could occur successfully.

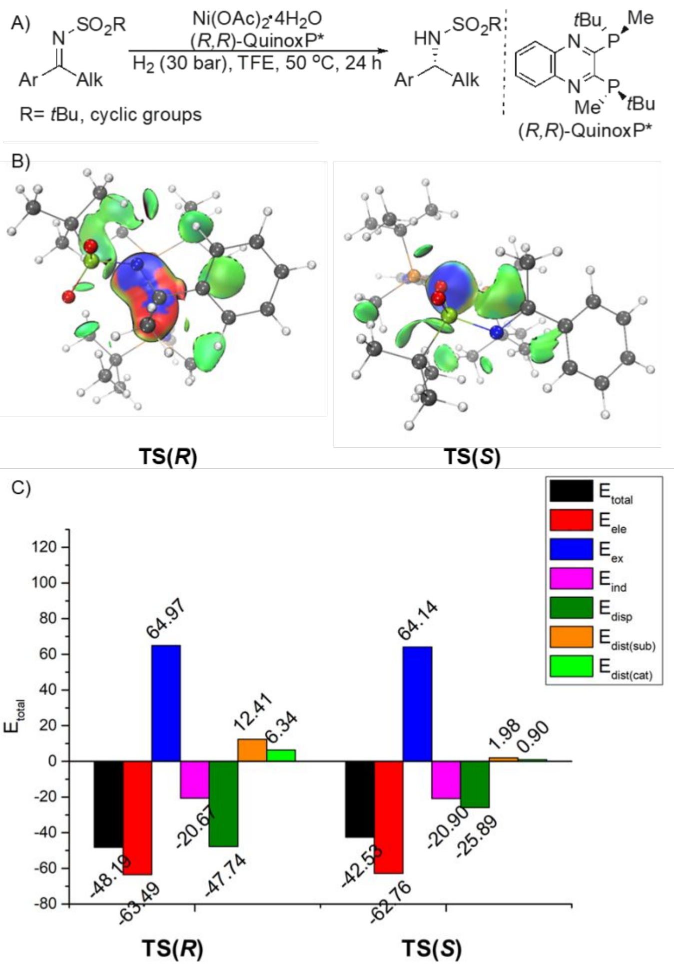

Figure 5. A) Hydrogenation of *N*-sulfonyl imines; B) IGM analysis of **TS(*R*)** and **TS(*S*)**; C) EDA analysis of **TS(*R*)** and **TS(*S*)**.

In 2022, the W. Zhang group reported the development of an environmentally friendly, earth-abundant, transition-metal nickel catalyzed asymmetric hydrogenation of oximes, remaining challenge due to the labile N-O bond and sluggish C=N bond (Figure 6A).[15] By employing a readily available (*S*,*S*)-Ph-BPE-Ni complex catalyst, the hydrogenation of oximes proceeded smoothly to enantiomerically enriched hydroxylamines with up to 99% yield, 99% ee and with 1000 S/C. Normal aryl-substituted diphosphine ligand with axial chirality like (*S*)-BINAP or (*S*)-Segphos gave desired product with low yield as well (7% and 50%, respectively). The ligand with phospholane skeleton like (*S*,*S*)-Ph-BPE behaved well. DFT computation results indicated that the hydrogenation efficiency and enantioselectivity were facilitated by multiple weak interactions between the Ni-catalyst and oxime substrate. In Zhang's work, weak attractive interactions were found in the structures of **TS(*R*)** and **TS(*S*)**, playing crucial roles by lowering the reaction barriers, thus raising the reaction efficiency. We found that because only non-polar groups exist in the ligand, no obvious hydrogen bond with hydroxyl group was observed. Instead, there are a lot of C-H···H-C and C-H···π interactions between substrates and catalysts in the IGM analysis (Figure 6B).

The EDA shows stronger dispersion interactions than the induction interactions (Figure 6C), exhibiting the importance of dispersion interactions between substrates and metal catalysts. Though **TS(*S*)** with the lower activation energy in Figure 6 has a relatively weaker attractive dispersion interaction (E_{disp} = -44.3 kcal/mol) than that of **TS(*R*)** (E_{disp} = -48.1 kcal/mol), without these dispersion interactions provided from the special phospholane skeleton, the reaction did not occur smoothly.

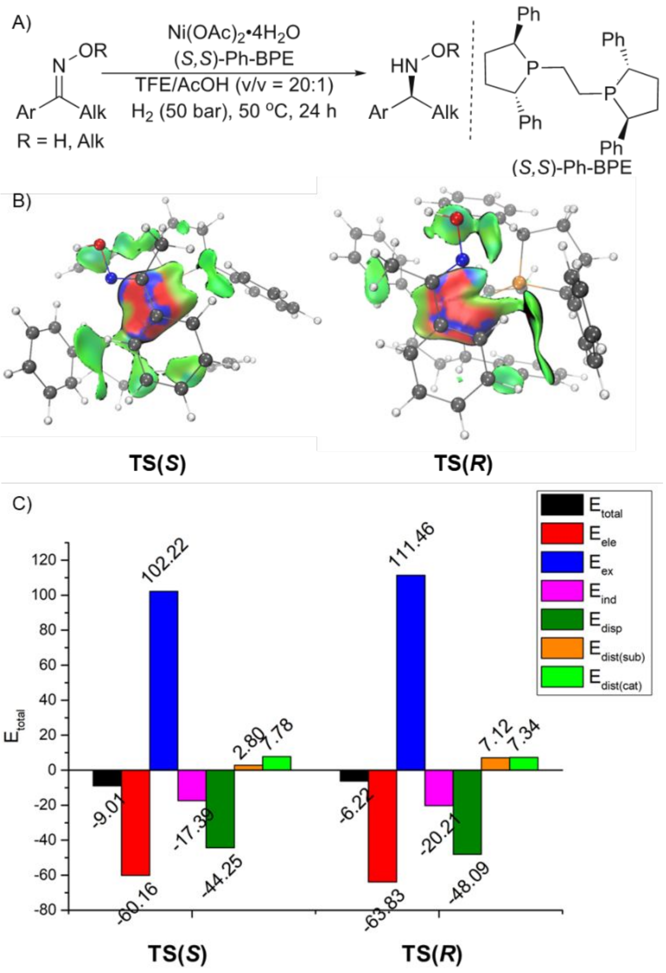

Figure 6. A) Hydrogenation of oximes; B) IGM analysis of **TS(*S*)** and **TS(*R*)**; C) EDA analysis of **TS(*S*)** and **TS(*R*)**.

Very recently, the W. Zhang group reported another efficient nickel catalyzed asymmetric hydrogenation of α-substituted vinylphosphonates and diarylvinylphosphine oxides, affording corresponding chiral α-substituted ethylphosphonate and ethylphosphine oxide compounds with 99% yield, 96% ee and 1000 S/C, which are widely used in drugs, pesticides, and ligands (Figure 7A).[16] The hydrogenation reactivity was high even with aryl-substituted ligands. However, the enantioselectivity of the reaction showed it was sensitive to the alkyl group of the phosphate (R group in Figure 7A). The ee increased from 88% to 91% when switching the R group from OEt to O^{i}Pr, indicating that dispersion interactions increase the enantioselectivity. Zhang's DFT calculation shows that the weak attractive interactions between the catalyst and the terminal olefin substrate in **TS(*R*)** are greater than those in **TS(*S*)**, which play important roles in the transition states and could lower the barrier of reduction for the olefins.

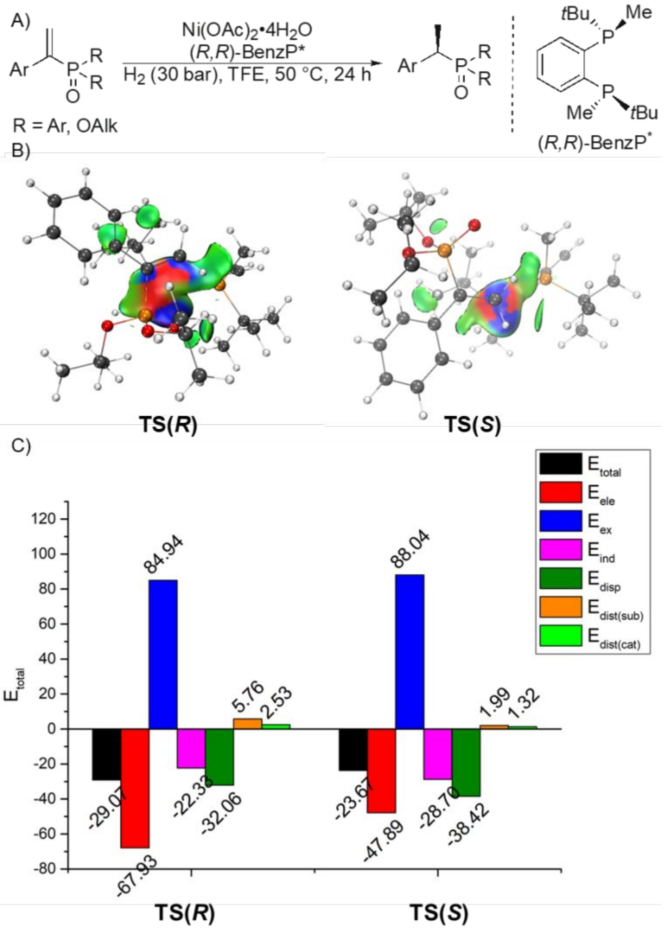

Figure 7. A) Hydrogenation of diisopropyl (1-phenylvinyl)phosphonate; B) IGM analysis of **TS(*R*)** and **TS(*S*)**; C) EDA analysis of **TS(*R*)** and **TS(*S*)**.

According to our IGM analysis, interactions between the *tert*-butyl group on the ligand and benzyl group of the substrate and the interactions between the *tert*-butyl group on the ligand and isopropyl group of the substrate guarantee the lower energy of **TS(*R*)**, benefiting from the *tert*-butyl group of the ligand (Figure 7B). This reflects the stronger dispersion energies compared with induction energies in EDA (Figure 7C), thus increase the reactivity. Though **TS(*R*)** with the lower activation energy in Figure 7 has a relatively weaker attractive dispersion interaction (E_{disp} = -32.1 kcal/mol) than that of **TS(*S*)** (E_{disp} = -38.4 kcal/mol), the additional Ni-O bond provided extra stabilization energy (E_{ele}). However, this additional bond is not affected by the R group of the phosphate. Even if there was influence, the larger steric hindrance of the R group (O^{i}Pr) should weaken this bond, yet the O^{i}Pr increase the ee value. Without the larger alkyl group, the difference of E_{disp} between two transition states could be larger; the dispersion interaction increased enantioselectivity in this case. On the other hand, when using aryl-substituted ligands with the same C_2 symmetry, the reaction gave desired products with low enantioselectivity (63%-82% ee), indicating that the dispersion interactions promoted the enantioselectivity. Both Zhang's DFT computational result and our IGM/EDA analysis indicated the dominance of dispersion interactions, and are consistent with the experimental data mentioned above.

Conclusions

Our IGM/EDA analysis further demonstrates that the Zhang group has discovered an important role of weak attractive interactions in asymmetric catalytic hydrogenations, which provides a new strategy for the sophisticated design of chiral transition metal catalysts involving both noble and earth-abundant metals. In addition, we show that the dispersion interactions activate the asymmetric hydrogenation reaction by the favorable interaction between substrate and metal catalyst. Based on these interactions, W. Zhang and coworkers developed several highly efficient asymmetric hydrogenations of *N*-sulfonyl imines, *α*-formyl enamides, oximes and α-substituted vinylphosphonates using chiral transition-metal catalysts derived from noble to earth-abundant metals, producing the corresponding chiral compounds with high yields, enantioselectivities, and S/C ratios.

Conflicts of interest

The authors declare no conflict of interest.

Acknowledgements

We gratefully acknowledge the National Science Foundation (CHE-1764328 to K.N.H.), the National Natural Science Foundation of China (Grant 22271071 to L.Y.), and the Natural Science Foundation of Zhejiang Province (Grant LY20B020010 to L.Y.) for financial support.

References

1 J. P. Wagner, P. R. Schreiner, London Dispersion in Molecular Chemistry-Reconsidering Steric Effects, *Angew. Chem. Int. Ed.* 2015, **54**, 12274–12296.
2 M. Bursch, E. Caldeweyher, A. Hansen, H. Neugebauer, S. Ehlert, S. Grimme, Understanding and Quantifying London Dispersion Effects in Organometallic Complexes, *Acc. Chem. Res.* 2019, **52**, 258-266.
3 P. H.-Y. Cheong, C. Y. Legault, J. M. Um, N. Çelebi-Ölçüm, K. N. Houk, Quantum Mechanical Investigations of Organocatalysis: Mechanisms, Reactivities, and Selectivities, *Chem. Rev.*, 2011, **111**, 5042–5137.
4 S. E. Wheeler, T. J. Seguin, Y. Guan, A. C. Doney, Noncovalent Interactions in Organocatalysis and the Prospect of Computational Catalyst Design, *Acc. Chem. Res.*, 2016, **49**, 1061–1069.
5 G. Lu, R. Y. Liu, Y. Yang, C. Fang, D. S. Lambrecht, S. L. Buchwald, P. Liu, Ligand–Substrate Dispersion Facilitates the Copper-Catalyzed Hydroamination of Unactivated Olefins, *J. Am. Chem. Soc.*, 2017, **139**, 16548–16555.
6 B, Li, H. Xu, Y. Dang, K. N. Houk, Dispersion and Steric Effects on Enantio-/Diastereoselectivities in Synergistic Dual Transition-Metal Catalysis, *J. Am. Chem. Soc.*, 2022, **144**, 1971–1985.

7 H. Wang, J. Wen, X. Zhang, Chiral Tridentate Ligands in Transition Metal-Catalyzed Asymmetric Hydrogenation, *Chem. Rev.*, 2021, **121**, 7530—7567.

8 K. Püntener, M. Scalone, In Enantioselective Hydrogenation: Applications in Process R&D of Pharmaceuticals, (Eds: H. U. Blaser, H. J. Federsel), Wiley-VCH, Weinheim, Germany 2010, CH 2.

9 J. Wen, F. Wang, X. Zhang, Asymmetric Hydrogenation Catalyzed by First-row Transition Metal Complexes, *Chem. Soc. Rev.* 2021, **50**, 3211—3237.

10 J. Chen, Z. Zhang, B. Li, F. Li, Y. Wang, M. Zhao, I. D. Gridnev, T. Imamoto, W. Zhang, $Pd(OAc)_2$-Catalyzed Asymmetric Hydrogenation of Sterically Hindered *N*-tosylimines, *Nat. Commun.*, 2018, **9**, 5000.

11 J. Zhang, J. Jia, X. Zeng, Y. Wang, Z. Zhang, I. D. Gridnev, W. Zhang, Chemo- and Enantioselective Hydrogenation of α-Formyl Enamides: An Efficient Access to Chiral α-Amido Aldehydes, *Angew. Chem. Int. Ed.*, 2019, **58**, 11505–11512.

12 B. Li, J. Chen, Z. Zhang, I. D. Gridnev, W. Zhang, Ni-Catalyzed Asymmetric Hydrogenation of N-Sulfonyl Imines, *Angew. Chem. Int. Ed.*, 2019, **58**, 7329–7334.

13 Y. Hu, J. Chen, B. Li, Z. Zhang, I. D. Gridnev, W. Zhang, Nickel-Catalyzed Asymmetric Hydrogenation of 2-Amidoacrylates, *Angew. Chem. Int. Ed.*, 2020, **59**, 5371–5375.

14 D. Liu, B. Li, J. Chen, I. D. Gridnev, D. Yan, W. Zhang, Ni-Catalyzed Asymmetric Hydrogenation of *N*-Aryl Imino Esters for the Efficient Synthesis of Chiral α-Aryl Glycines, *Nat. Commun.*, 2020, **11**, 5935.

15 B. Li, J. Chen, D. Liu, I. D. Gridnev, W. Zhang, Nickel-Catalysed Asymmetric Hydrogenation of Oximes, *Nat. Chem.*, 2022, **14**, 920–927.

16 H. Wei, H. Chen, J. Chen, I. D. Gridnev, W. Zhang, Nickel-Catalyzed Asymmetric Hydrogenation of α-Substituted Vinylphosphonates and Diarylvinylphosphine Oxides, *Angew. Chem. Int. Ed.*, 2023, **62**, e202214990.

17 C. Lefebvre, G. Rubez, H. Khartabil, J.-C. Boisson, J. Contreras-García, E. Hénon, Accurately Extracting the Signature of Intermolecular Interactions Present in the NCI Plot of the Reduced Density Gradient Versus Electron Density, *Phys. Chem. Chem. Phys.* 2017**, 19**, 17928–17936.

18 For selected papers using IGM analysis: a) W. Liu, C. L. Stern, J. F. Stoddart, Suit[4]ane, *J. Am. Chem. Soc.* 2020**, 142**, 10273–10278; b) S. Gao, M. Duan, L. R. Andreola, P. Yu, S. E. Wheeler, K. N. Houk, M. Chen, Unusual Enantiodivergence in Chiral Brønsted Acid-Catalyzed Asymmetric Allylation with β-Alkenyl Allylic Boronates. *Angew. Chem. Int. Ed.* 2022**, 61**, e202208908; c) W. Zhang, L. Chen, S. Dai, C. Zhao, C. Ma, L. Wei, M. Zhu, S. Y. Chong, H. Yang, L. Liu, Y. Bai, M. Yu, Y. Xu, X.-W. Zhu, Q. Zhu, S. An, R. S. Sprick, M. A. Little, X. Wu, S. Jiang, Y. Wu, Y.-B. Zhang, H. Tian, W.-H. Zhu, A. I. Cooper, Reconstructed Covalent Organic Frameworks, *Nature* 2022**, 604**, 72–79.

19 E. R. Johnson, S. Keinan, P. Mori-Sánchez, J. Contreras-García, A. J. Cohen, W. Yang, Revealing Noncovalent Interactions, *J. Am. Chem. Soc.* 2010**, 132**, 6498–6506.

20 Jeziorski, B.; Moszynski, R.; Szalewicz, K., Perturbation Theory Approach to Intermolecular Potential Energy Surfaces of van der Waals Complexes. *Chemical Reviews* 1994**, 94**, 1887-1930.

21 Chen, J.; Gridnev, I. D., Size is Important: Artificial Catalyst Mimics Behavior of Natural Enzymes. *iScience* 2020**, 23**, 100960.

22 Chen, J.; Liu, D.; Butt, N.; Li, C.; Fan, D.; Liu, Y.; Zhang, W., Palladium-Catalyzed Asymmetric Hydrogenation of α-Acyloxy-1-arylethanones. *Angew. Chem. Int. Ed.*, 2013, **52**, 11632-11636.